ELSEVIER

Journal of Chromatography A, 908 (2001) 35–47

JOURNAL OF CHROMATOGRAPHY A

www.elsevier.com/locate/chroma

Pore network modelling: determination of the dynamic profiles of the pore diffusivity and its effect on column performance as the loading of the solute in the adsorbed phase varies with time

J.J. Meyers, O.K. Crosser, A.I. Liapis*

Department of Chemical Engineering and Biochemical Processing Institute, University of Missouri-Rolla, Rolla, MO 65409-1230, USA

Abstract

A three-dimensional pore network model for diffusion in porous adsorbent particles was employed in a dynamic adsorption model that simulates the adsorption of a solute in porous particles packed in a chromatographic column. The solution of the combined model yielded the dynamic profiles of the pore diffusion coefficient of β-galactosidase along the radius of porous ion-exchange particles and along the length of the column as the loading of the adsorbate molecules on the surface of the pores occurred, and, the dynamic adsorptive capacity of the chromatographic column as a function of the design and operational parameters of the chromatographic system. The pore size distribution of the porous adsorbent particles and the chemistry of the adsorption sites were unchanged in the simulations. It was found that for a given column length the dynamic profiles of the pore diffusion coefficient were influenced by: (i) the superficial fluid velocity in the column, (ii) the diameter of the adsorbent particles and (iii) the pore connectivity of the porous structure of the adsorbent particles. The effect of the magnitude of the pore connectivity on the dynamic profiles of the pore diffusion coefficient increased as the diameter of the adsorbent particles and the superficial fluid velocity in the column increased. The dynamic adsorptive capacity of the column increased as: (a) the particle diameter and the superficial fluid velocity in the column decreased, and (b) the column length and the pore connectivity increased. In preparative chromatography, it is desirable to obtain high throughputs within acceptable pressure gradients, and this may require the employment of larger diameter adsorbent particles. In such a case, longer column lengths satisfying acceptable pressure gradients with adsorbent particles having higher pore connectivity values could provide high dynamic adsorptive capacities. An alternative chromatographic system could be comprised of a long column packed with large particles which have fractal pores (fractal particles) that have high pore connectivities and which allow high intraparticle diffusional and convective flow mass transfer rates providing high throughputs and high dynamic adsorptive capacities. If large scale monoliths could be made to be reproducible and operationally stable, they could also offer an alternative mode of operation that could provide high throughputs and high dynamic adsorptive capacities.

Keywords: Network model; Pore size distribution; Pore diffusion; Dynamic adsorption; Pore connectivity; Preparative chromatography; Pore structure; Galactosidase; Proteins

1. Introduction

In the study of systems involving the diffusion and adsorption of an adsorbate A in porous chromatographic particles, it is very important to determine quantitatively the dependence of the pore diffusion coefficient, D_p, of adsorbate A on: (a) the pore structure of the adsorbent particles, (b) the molecular size of the adsorbate molecules and of the adsorption sites (ligands) on the surface of the pores, and (c) the

*Corresponding author. Fax: +1-573-3412-071.

0021-9673/01/$ – see front matter
PII: S0021-9673(00)00795-0

fractional saturation of the adsorption sites. Liapis and co-workers [1–5] have constructed pore network models which were utilized to simulate intraparticle fluid flow and pore diffusion of adsorbate molecules in porous chromatographic particles packed in a column or in monoliths; the flowing fluid stream in the packed column or in the monolith could be driven by an applied pressure gradient or by an applied electric field (electroosmotic flow). In their pore network models the combined effects of steric hindrance at the entrance to the pores and frictional resistance within the pores, as well as the effects of pore size distribution, pore connectivity of the pore structure of the adsorbent particles, molecular size of the adsorbate molecules and of the adsorption sites (ligands), and the fractional saturation of the adsorption sites have been considered. Thus, the value of the pore diffusion coefficient, D_p, of adsorbate A in porous adsorbent particles or in a monolith could be determined as the process of adsorption occurs by the pore network modeling theory presented in the work of Liapis and co-workers [1–3]

In this work, the effect on column performance of the diffusion of molecules in porous chromatographic adsorbents is studied for column systems involving frontal chromatography of large adsorbate molecules.

2. Theoretical formulation

In this work, the dynamic adsorption mechanism is considered to be described by the following second-order reversible interaction mechanism [6]:

$$\frac{\partial C_s}{\partial t} = k_1 C_p (C_T - C_s) - k_2 C_s \quad (1)$$

If

$$\theta (\theta = C_s / C_T)$$

is taken to represent the fractional saturation of the adsorption sites, then Eq. (1) takes the following form in terms of the variable θ:

$$\frac{\partial \theta}{\partial t} = k_1 C_p (1 - \theta) - k_2 \theta \quad (2)$$

It is worth noting at this point that at equilibrium:

$$(\partial C_s / \partial t = \partial \theta / \partial t = 0)$$

Eqs. (1) and (2) provide the functional form of the Langmuir isotherm. At equilibrium, Eq. (1) becomes

$$C_s = \frac{K C_T C_p}{1 + K C_p} \quad (3)$$

while Eq. (2) takes the following form:

$$\theta = \frac{K C_p}{1 + K C_p} \quad (4)$$

In Eqs. (1)–(4), the variable C_p represents the concentration of adsorbate A in the pore fluid, C_s denotes the concentration of adsorbate A in the adsorbed phase, C_T represents the maximum concentration of adsorbate A in the adsorbed phase, k_1 and k_2 are the rate constants of the adsorption and desorption steps, respectively and $K (K = k_1/k_2)$ is the equilibrium constant.

By employing Eq. (2) or Eq. (4) and the pore network modeling theory presented in the works of Liapis and co-workers [1–3], the pore diffusion coefficient, D_p, of adsorbate A can be determined in the porous adsorbent particles for $0 \leq \theta \leq 1$, when the pore size distribution (PSD) and pore connectivity, n_T, of the porous adsorbent particles are known [1–5]. In this work, Adsorbent I of Ref. [2] is taken to represent the porous ion-exchange particles in which the molecules of β-galactosidase (adsorbate) are adsorbed. The pore size distribution of the porous adsorbent particles and the chemistry of the adsorption sites were unchanged in the simulations. The PSD of the porous adsorbent particles employed in this work is the same as the PSD of Adsorbent I presented in Ref. [2]. The mathematical expression of the PSD is:

$$f(d_{pore}) = \sum_{i=1}^{2} \left(\frac{\gamma_i}{\sqrt{2\pi}\sigma_i} \right) \cdot \exp \left[-\frac{1}{2} \cdot \left(\frac{d_{pore} - \mu_i}{\sigma_i} \right)^2 \right] \quad (5)$$

This pore size distribution (PSD) is made up of the sum of two Gaussian distributions in order to represent the intraparticle micropores ($i = 1$) and the intraparticle macropores ($i = 2$). The values of γ_1 and γ_2 are 2.0 and 2.48 and represent the relative proportions of the micropores and macropores, respectively. The parameter d_{pore} represents the pore diameter, μ_i ($i = 1, 2$) denotes the mean diameter of

pores of class i and σ_i ($i=1$, 2) is the standard deviation of the diameter of pores of class i. The values of μ_i and σ_i in Eq. (5) are as follows: $\mu_1=0.039$ μm; $\mu_2=0.534$ μm; $\sigma_1=0.03$ μm; and $\sigma_2=0.38$ μm. The function $f(d_{pore})$ provides the number of pores having diameter d_{pore}. The value of the porosity, ϵ_p, of the porous particles at time $t=0$ is equal to 0.50, the thickness of the layer of the adsorption sites on the surface of the pores of the ion-exchange particles is taken to be [2] approximately equal to zero, the value of the effective molecular radius, α_1, of β-galactosidase is taken to be equal to 70.6 Å, and the magnitude of the free molecular diffusion coefficient, D_{mf}, of β-galactosidase is $3.9\cdot10^{-11}$ m^2/s. In Fig. 1, the values of the pore diffusion coefficient, D_p, of the β-galactosidase (adsorbate) molecules in the adsorbent particles are presented for different values of the pore connectivity, n_T, of the porous structure of the adsorbent particles and when the magnitude of the fractional saturation, θ, of the adsorption sites is varied from $\theta=0$ to $\theta=1$. The results in Fig. 1 have been obtained from the pore network modeling theory presented in Ref. [2]. The results in Fig. 1 clearly indicate that D_p increases as n_T increases and θ decreases. Then the experimental functions of θ that were constructed [7] to represent the pore diffusivity data in Fig. 1 were employed in the mathematical model of McCoy and Liapis [6] that simulates the dynamic behavior of frontal chromatography in

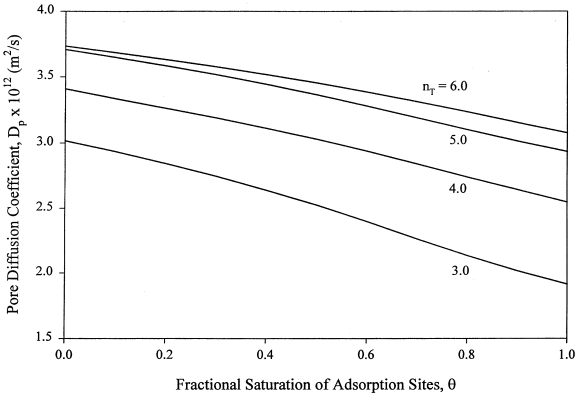

Fig. 1. Pore diffusion coefficient, D_p, of β-galactosidase as a function of the fractional saturation, θ, of the adsorption sites within ion-exchange particles having values of pore connectivity, n_T, of 3.0, 4.0, 5.0 and 6.0.

columns packed with porous adsorbent particles or in monoliths [3], in order to determine the pore diffusion coefficient, D_p, of β-galactosidase at different positions along the radius of the particles and along the axis of the column. The dynamic behavior of the frontal chromatography of β-galactosidase was obtained in this work by solving the dynamic model of adsorption in chromatographic columns developed by McCoy and Liapis [6]. This model [6] accounts for the following mass transfer mechanisms: (i) bulk fluid flow of adsorbate in the flowing fluid stream of the column, (ii) axial dispersion of adsorbate in the flowing fluid stream of the column, (iii) film mass transfer of adsorbate (mass transfer of adsorbate through the liquid film surrounding the porous adsorbent particles), (iv) diffusion of adsorbate in the liquid in the pores of the porous adsorbent particles (pore diffusion) and (v) the adsorption mechanism between the adsorbate molecules and the adsorption sites on the surface of the pores of the adsorbent particles. The adsorption mechanism between the β-galactosidase molecules and the adsorption sites [mass transfer mechanism (v)] was considered to be described by the second order reversible interaction expression given in Eq. (2). The values of the other parameters used in the column model of McCoy and Liapis [6] to obtain the results presented in this work, are as follows: $C_{d,in}=0.1$ kg/m^3; $C_T=2.2$ kg/m^3; $D_L=0$; $k_1=2.35\cdot10^{-2}$ $m^3/(kg\ s)$; $k_2=5.17\cdot10^{-6}$ s^{-1}; $\epsilon=0.36$. The value of the film mass transfer coefficient, K_f, for different values of V_f and r_p is obtained from Eq. (6)

$$K_f\,|_{V_f,\,r_p>7.5\cdot10^{-6}\,m} = K_f\,|_{V_f,\,r_p=7.5\cdot10^{-6}\,m} \cdot\left[\frac{7.5\cdot10^{-6}\,m}{r_p}\right]^{2/3} \quad (6)$$

where

$$K_f\,|_{V_f,\,r_p=7.5\cdot10^{-6}\,m} = 5.275\cdot10^{-4}V_f^{1/3} \quad (7)$$

The units for K_f, r_p and V_f in Eqs. (6) and (7) are m/s, m and m/s, respectively. Five different column lengths were studied in this work such that the length of the column, L, was taken to be 0.1 m, 0.2 m, 0.3 m, 0.4 m and 0.5 m while the magnitude of the superficial velocity, V_f, in the column was varied from 100 to 1000 cm/h Adsorbent particles with

diameters, d_p, of 15 μm, 30 μm, 50 μm and 100 μm were employed in the simulations and the values of the pore connectivity, n_T, of the porous structure of the adsorbent particles studied in this work were $n_T = 3.0$, $n_T = 4.0$, $n_T = 6.0$ (the coordination number [1–3,5,8] of the three-dimensional pore network model [2] used in this work is six). The value of the axial dispersion coefficient, D_L, was taken to be zero because the estimated value of D_L from expressions presented in Heeter and Liapis [9] is so low that the error introduced, by setting D_L equal to zero in the model of McCoy and Liapis [2], in the calculated dynamic behavior of the column systems [9] is insignificant.

3. Results and discussion

In Figs. 2 and 3, the profiles of the pore diffusion coefficient, D_p, of β-galactosidase at the center and surface of the adsorbent particles and along the dimensionless length, x/L, of a column having a length $L = 0.5$ m, are presented at a time $t = t_b$ where 5% of breakthrough $[C_d(t = t_b,\ x = L)/C_{d,in} = 0.05]$ occurs (the values of t_b are shown in Fig. 6) and for different values of the pore connectivity, n_T, and of the particle diameter, d_p, and when the values of the superficial fluid velocity, V_f, are 300 cm/h and 500 cm/h, respectively. The results clearly indicate that, for a given set of values of V_f and n_T, and as the loading, θ, of the particles increases with decreasing particle diameter, d_p, (since a decreasing particle diameter provides a smaller diffusional path length for the same value of the pore connectivity, n_T [1,2]), the pore diffusivity, D_p, is lower (since the value of D_p decreases with increasing loading, θ, of the particles as shown in Fig. 1) along larger sections of the column. Also, the differences between the values of D_p at $r = r_p$ ($r_p = d_p/2$) and $r = 0$ are much smaller when the value of d_p decreases, because the loading, θ, of the particles with a smaller diameter occurs faster and is higher in magnitude and more uniform with respect to space when compared with the loading, θ, obtained in particles with larger diameters, and leads to values of D_p that can vary insignificantly with respect to the radial position, r, in the particles, while the variation of D_p in the axial direction of the column along the length of the column where the adsorption front has passed is significantly smaller when the particles packed in the column have small diameters. Furthermore, the results in Figs. 2 and 3 indicate that, for a given set of values of V_f and d_p, the pore diffusion coefficient, D_p, increases with increasing pore connectivity, n_T, the differences between the values of D_p at $r = r_p$ and $r = 0$ decrease as the value of n_T increases, and the magnitude of D_p is higher for larger values of x/L along the length of the column, for a given radial position in the particle, with increasing values of n_T. Also, by comparing the results in Figs. 2 and 3, it can be observed that as the value of the superficial fluid velocity, V_f, increases and reduces the residence time of the flowing fluid stream in the column, the loading, θ, of the particles packed in the column could maintain a high magnitude and be more uniform with respect to space (along the radial position, r, in the particles and along the axial direction, x, of the column) when the adsorbent particles have small diameters and the pore structure of the adsorbent particles has a high pore connectivity, n_T, value.

In Figs. 4–6, the time, t_b, at 5% breakthrough of β-galactosidase is shown for column lengths, L, of 0.2 m, 0.3 m and 0.5 m, respectively, where in each case the pore connectivity, n_T, has values of 3.0, 4.0 and 6.0, the particle diameter, d_p, has magnitudes of 15 μm, 30 μm, 50 μm and 100 μm, and the superficial fluid velocity, V_f, is varied from 100 cm/h to 1000 cm/h The results show that for a given set of values of L, d_p, and n_T, the time t_b decreases as the value of V_f increases because the higher values of V_f produce lower residence times in the column for the adsorbate molecules to penetrate into the pores of the adsorbent particles. Similarly, for a given set of values of V_f, d_p, and n_T, the time t_b decreases as the column length, L, decreases because the lower values of L provide smaller residence times in the column for the adsorbate molecules to penetrate into the pores of the adsorbent particles. Furthermore, for a given set of values of V_f, L, and n_T, the time t_b decreases as the magnitude of the particle diameter, d_p, increases because a larger particle provides a longer diffusional path length which leads to a smaller diffusional velocity [1,2,10] v_D, ($v_D = D_p/r_p$), and higher intraparticle mass transfer resistance to loading. The results in Figs. 4–6 also show that,

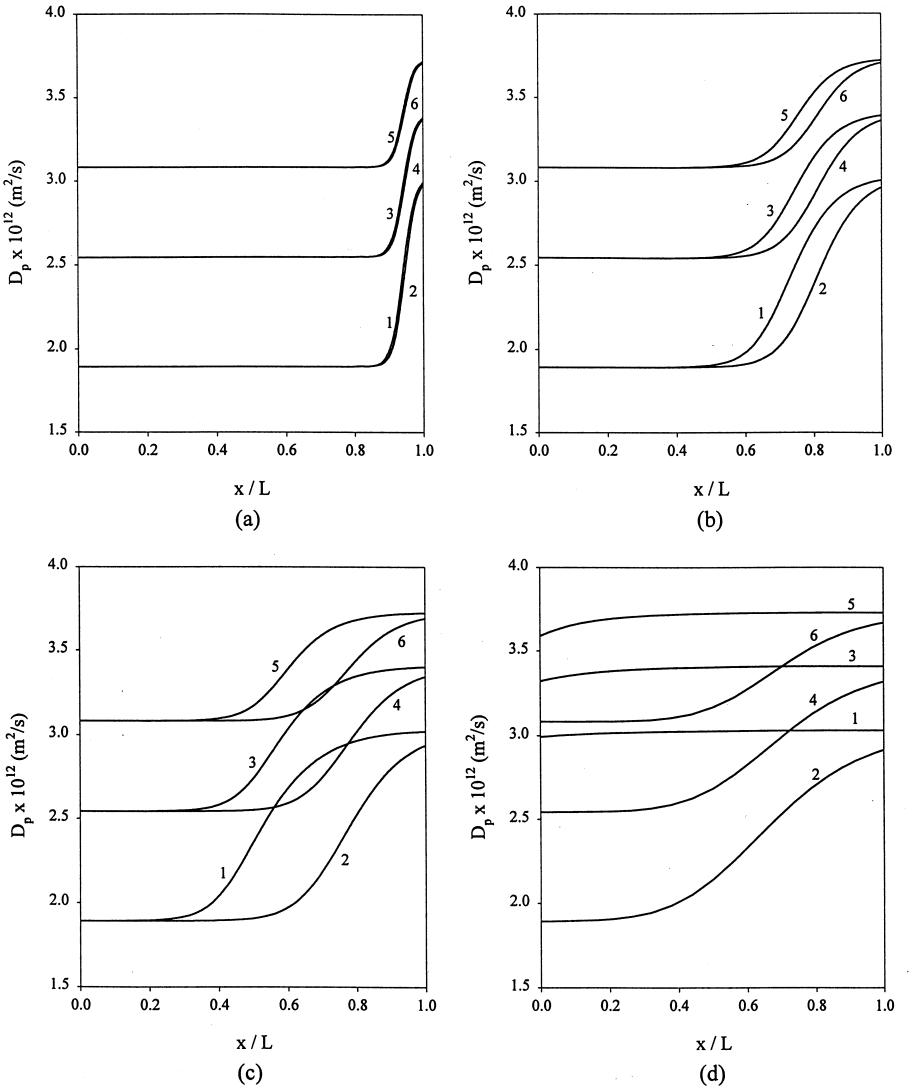

Fig. 2. Dynamic profiles of the pore diffusion coefficient, D_p, of β-galactosidase along the dimensionless length, x/L, of a column of length $L=0.5$ m at two different radial positions in the adsorbent particles and for three different values of the pore connectivity, n_T, at time $t=t_b$ when 5% breakthrough [$C_d(t=t_b, x=L)/C_{d,in}=0.05$] occurs and when the value of the superficial fluid velocity, V_f, is 300 cm/h. In: (a) $d_p=15$ μm; in (b) $d_p=30$ μm; in (c) $d_p=50$ μm; in (d) $d_p=100$ μm. The curves 1–6 in all cases denote the following: $1\equiv r=0$, $n_T=3.0$; $2\equiv r=r_p$, $n_T=3.0$; $3\equiv r=0$, $n_T=4.0$; $4\equiv r=r_p$, $n_T=4.0$; $5\equiv r=0$, $n_T=6.0$; $6\equiv r=r_p$, $n_T=6.0$.

for a given set of values of L, V_f and d_p, the time t_b increases as the magnitude of the pore connectivity, n_T, increases because a higher pore connectivity provides a lower intraparticle resistance to diffusion and leads to a higher loading rate. For a given set of values of L and V_f, the difference in the values of t_b obtained for different values of the pore connectivity, n_T, increases with increasing particle size, d_p; the exception to this result occurs when the magnitude of the superficial fluid velocity, V_f, is so high that this results in such a low residence time in the column that there is immediate breakthrough, since the

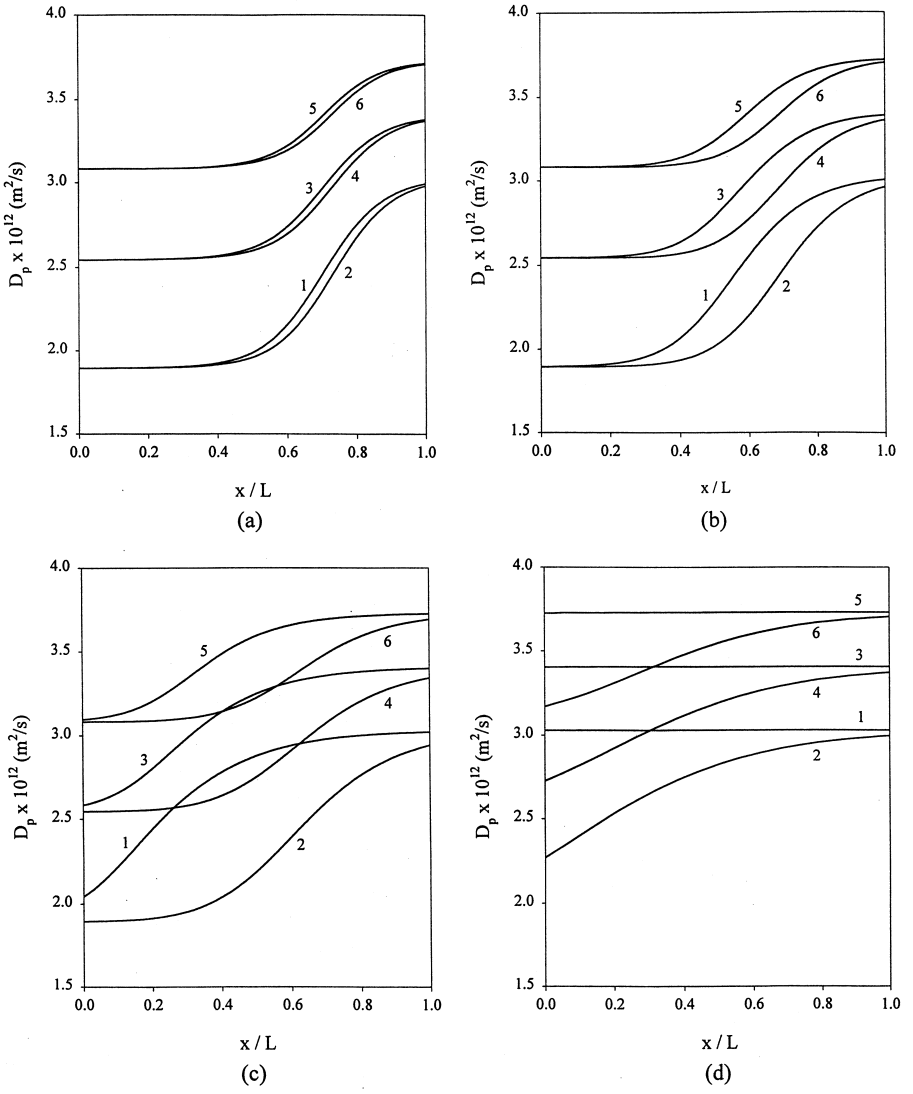

Fig. 3. Dynamic profiles of the pore diffusion coefficient, D_p, of β-galactosidase along the dimensionless length, x/L, of a column of length $L=0.5$ m at two different radial positions in the adsorbent particles and for three different values of the pore connectivity, n_T, at time $t=t_b$ when 5% breakthrough [$C_d(t=t_b, x=L)/C_{d,in}=0.05$] occurs and when the value of the superficial fluid velocity, V_f, is 500 cm/h. In: (a) $d_p=15$ μm; in (b) $d_p=30$ μm; in (c) $d_p=50$ μm; in (d) $d_p=100$ μm. The curves 1–6 in all cases denote the following: $1\equiv r=0$, $n_T=3.0$; $2\equiv r=r_p$, $n_T=3.0$; $3\equiv r=0$, $n_T=4.0$; $4\equiv r=r_p$, $n_T=4.0$; $5\equiv r=0$, $n_T=6.0$; $6\equiv r=r_p$, $n_T=6.0$.

penetration of adsorbate molecules in the adsorbent particles is too low. In this latter case, the difference in the values of t_b for different values of the pore connectivity, n_T, is much smaller than the differences obtained at lower values of V_f, as shown in Figs. 4–6, by the curves converging at higher values of V_f. The inset in each of the Figs. 4–6, shows an expanded view of the differences in t_b due to n_T at the higher values of V_f.

In Figs. 7–9, the dimensionless dynamic adsorptive capacity $M_{T,ads}/M^*_{T,ads}$ at 5% breakthrough is shown for superficial fluid velocities, V_f, of 100 cm/h, 300 cm/h, and 500 cm/h, respectively, where in each case the pore connectivity, n_T, has values of

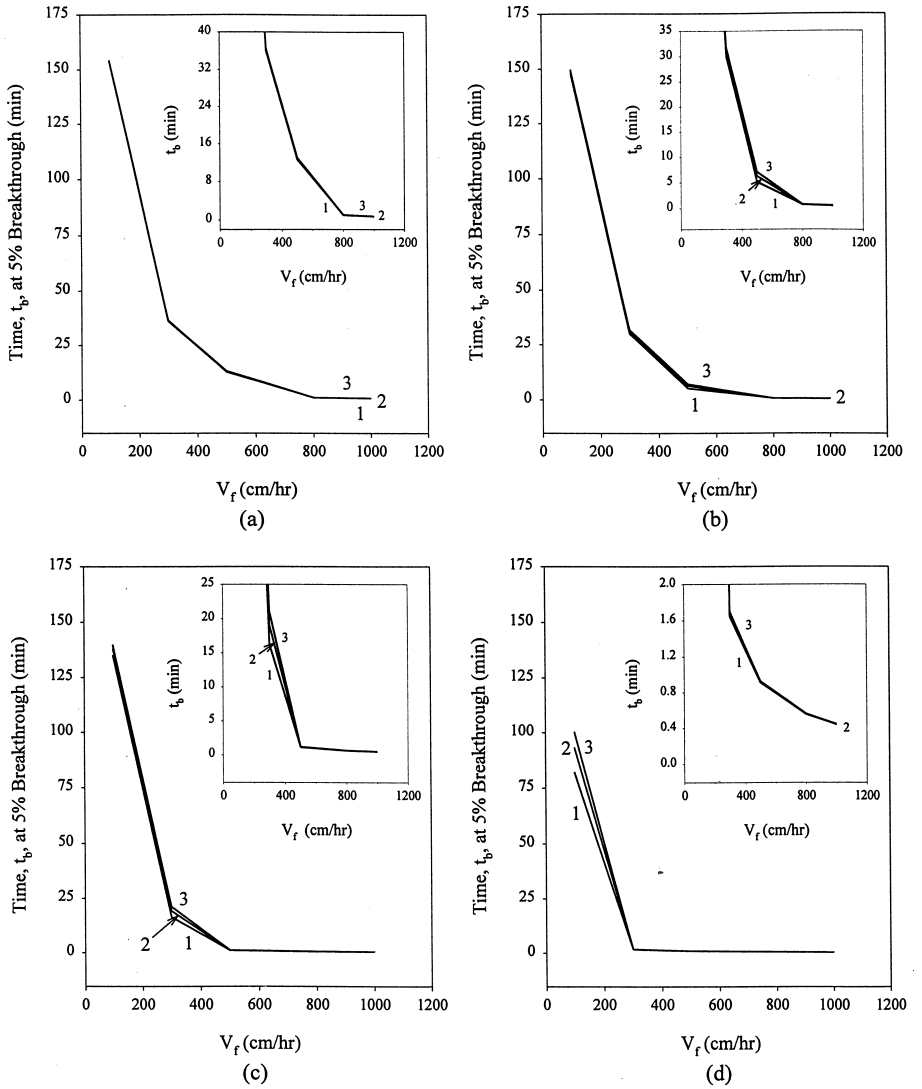

Fig. 4. Time t_b when 5% breakthrough [$C_d(t = t_b, x = L)/C_{d,in} = 0.05$] occurs as a function of the superficial fluid velocity, V_f, in the column at a column length, L, of 0.2 m for particle diameters, d_p, of 15 μm, 30 μm, 50 μm and 100 μm with the pore connectivity, n_T, equal to 3.0, 4.0 and 6.0. In: (a) $d_p = 15$ μm; in (b) $d_p = 30$ μm; in (c) $d_p = 50$ μm; in (d) $d_p = 100$ μm. The curves 1, 2 and 3 in all cases denote the following: $1 \equiv n_T = 3.0$; $2 \equiv n_T = 4.0$; $3 \equiv n_T = 6.0$.

3.0, 4.0 and 6.0, the particle diameter, d_p, has magnitudes of 15 μm, 30 μm, 50 μm and 100 μm and the column length, L, is varied from 0.1 m to 0.5 m. The results in Figs. 7–9 indicate that, for a given set of values of V_f, d_p and n_T, the value of $M_{T,ads}/M^*_{T,ads}$ increases as the column length, L, increases because the larger values of L provide longer residence times in the column for the adsorbate molecules to penetrate into the pores of the adsorbent particles. Furthermore, the results clearly show that for a given value of the column length, L, the dynamic adsorptive capacity $M_{T,ads}/M^*_{T,ads}$ increases as: (i) the superficial fluid velocity, V_f, decreases (a lower value of V_f provides, for a given value of L, a higher residence time in the column for the adsorbate molecules to penetrate into the pores of

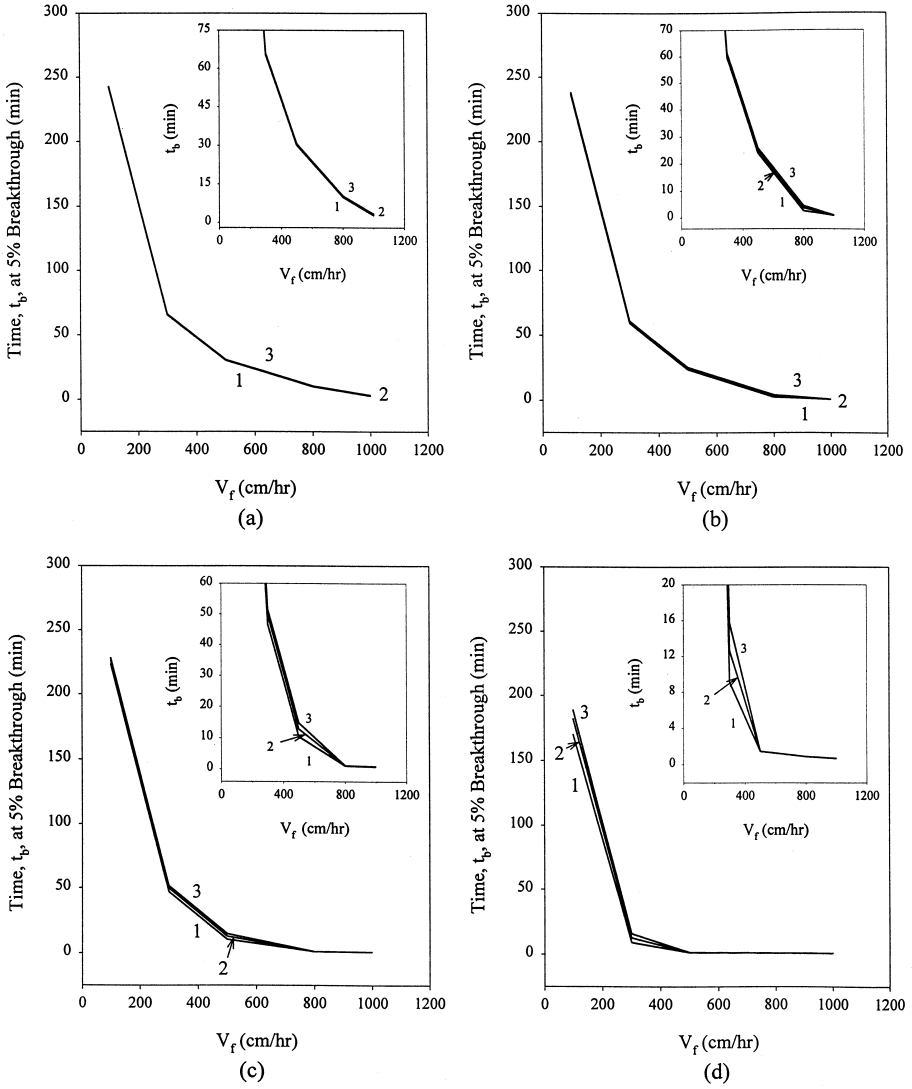

Fig. 5. Time t_b when 5% breakthrough [$C_d(t = t_b, x = L)/C_{d,in} = 0.05$] occurs as a function of the superficial fluid velocity, V_f, in the column at a column length, L, of 0.3 m for particle diameters, d_p, of 15 μm, 30 μm, 50 μm and 100 μm with the pore connectivity, n_T, equal to 3.0, 4.0 and 6.0. In: (a) $d_p = 15$ μm; in (b) $d_p = 30$ μm; in (c) $d_p = 50$ μm; in (d) $d_p = 100$ μm. The curves 1, 2 and 3 in all cases denote the following: $1 \equiv n_T = 3.0$; $2 \equiv n_T = 4.0$; $3 \equiv n_T = 6.0$.

the adsorbent particles), (ii) the particle diameter, d_p, decreases and (iii) the pore connectivity, n_T, increases. For lower values of V_f and d_p, the effect of the pore connectivity, n_T, on $M_{T,ads}/M^*_{T,ads}$ is very small and in such systems the curves 1, 2 and 3 that represent different values of n_T are almost indistinguishable from each another. But for higher values of V_f and d_p, the effect of n_T on $M_{T,ads}/M^*_{T,ads}$ can be very significant, as the results in Figs. 7–9 clearly show.

4. Conclusions and remarks

In this work, a three-dimensional pore network model for diffusion in porous adsorbent particles was

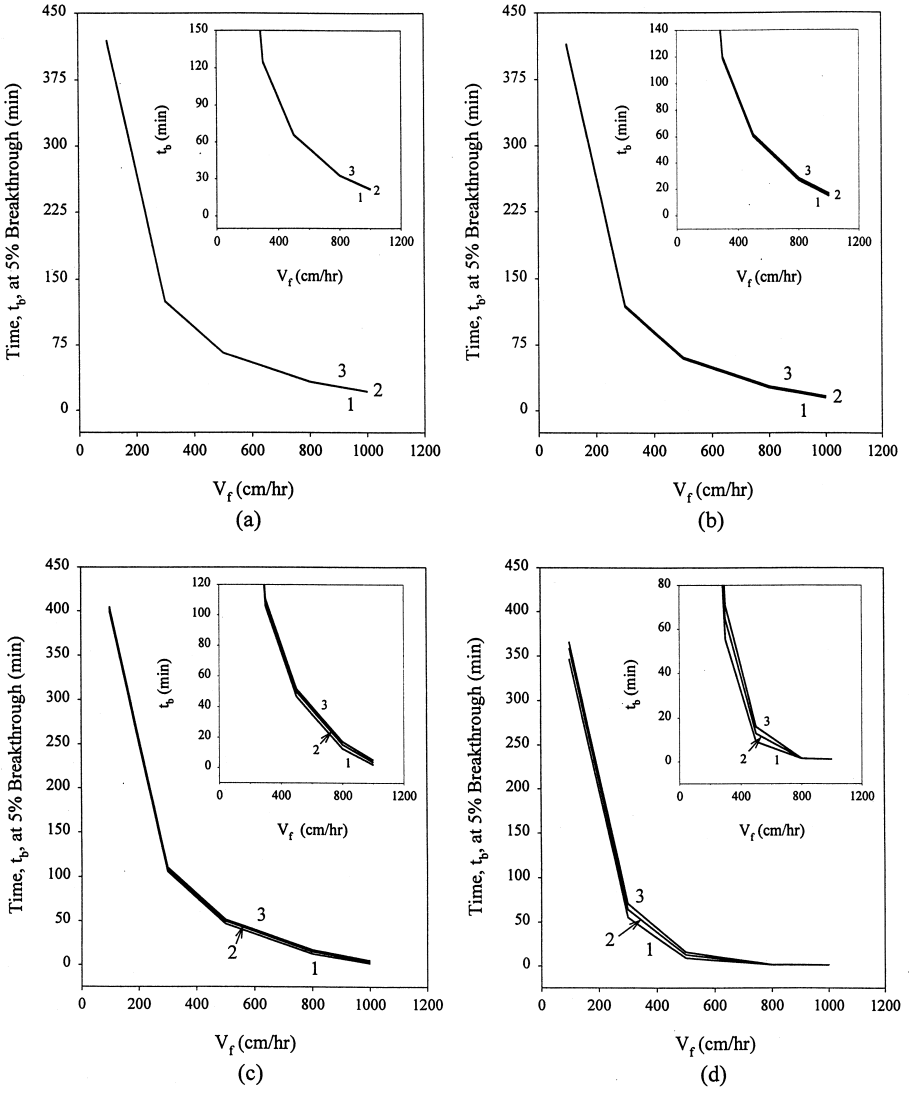

Fig. 6. Time t_b when 5% breakthrough [$C_d(t = t_b, x = L)/C_{d,in} = 0.05$] occurs as a function of the superficial fluid velocity, V_f, in the column at a column length, L, of 0.5 m for particle diameters, d_p, of 15 μm, 30 μm, 50 μm and 100 μm with the pore connectivity, n_T, equal to 3.0, 4.0 and 6.0. In: (a) $d_p = 15$ μm; in (b) $d_p = 30$ μm; in (c) $d_p = 50$ μm; in (d) $d_p = 100$ μm. The curves 1, 2 and 3 in all cases denote the following: $1 \equiv n_T = 3.0$; $2 \equiv n_T = 4.0$; $3 \equiv n_T = 6.0$.

employed in a dynamic adsorption model that simulates the adsorption of a solute in porous particles packed in a chromatographic column. The solution of the combined model made it possible to obtain for different values of the design and operational parameters of the chromatographic system, the dynamic profiles of the pore diffusion coefficient, D_p, of β-galactosidase along the radius of porous ion-exchange particles and along the length of the column as the loading of the adsorbate molecules on the surface of the pores occurred, and the dynamic adsorptive capacity, $M_{T,ads}/M^*_{T,ads}$, of the chromatographic column.

It was found that the dynamic profiles of the pore diffusion coefficient, D_p, of β-galactosidase, for a given column length, were influenced by: (i) the

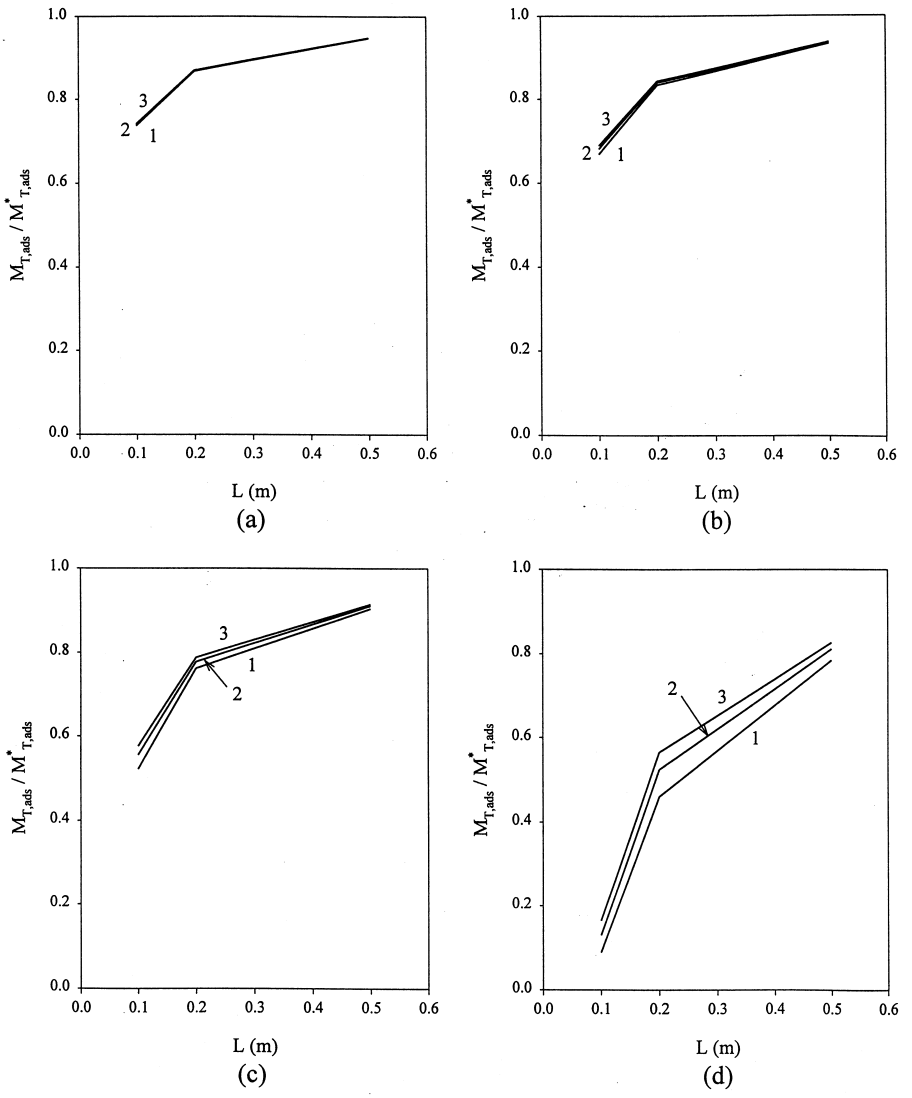

Fig. 7. Dynamic adsorptive capacity, $M_{T,ads}/M^*_{T,ads}$, of the column at time t_b when 5% breakthrough [$C_d(t = t_b, x = L)/C_{d,in} = 0.05$] occurs as a function of the column length, L, at a superficial fluid velocity, V_f, of 100 cm/h for particle diameters, d_p, of 15 μm, 30 μm, 50 μm and 100 μm with the pore connectivity, n_T, equal to 3.0, 4.0 and 6.0. In: (a) $d_p = 15$ μm; in (b) $d_p = 30$ μm; in (c) $d_p = 50$ μm; in (d) $d_p = 100$ μm. The curves 1, 2 and 3 in all cases denote the following: $1 \equiv n_T = 3.0$; $2 \equiv n_T = 4.0$; $3 \equiv n_T = 6.0$.

value of the superficial fluid velocity in the column, V_f, (ii) the magnitude of the diameter, d_p, of the adsorbent particles and (iii) the value of the pore connectivity, n_T, of the porous adsorbent particles; the effect of the magnitude of the pore connectivity, n_T, on the dynamic profiles of the pore diffusion coefficient, D_p, increased as the diameter, d_p, of the adsorbent particles and the superficial fluid velocity, V_f, in the column increased. The dynamic adsorptive capacity, $M_{T,ads}/M^*_{T,ads}$, of the column increased as: (a) the values of the particle diameter, d_p, and of the superficial fluid velocity, V_f, decreased and (b)

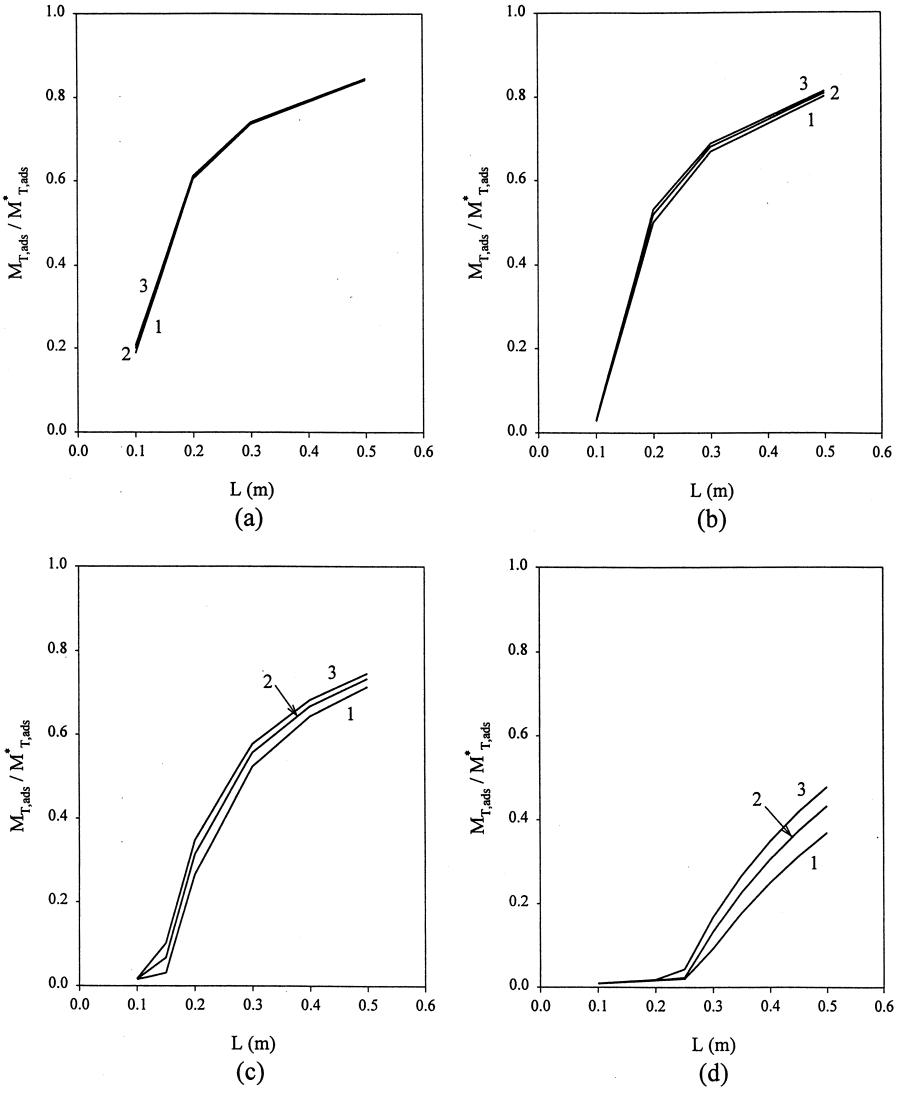

Fig. 8. Dynamic adsorptive capacity, $M_{T,ads}/M^*_{T,ads}$, of the column at time t_b when 5% breakthrough [$C_d(t = t_b, x = L)/C_{d,in} = 0.05$] occurs as a function of the column length, L, at a superficial fluid velocity, V_f, of 300 cm/h for particle diameters, d_p, of 15 μm, 30 μm, 50 μm and 100 μm with the pore connectivity, n_T, equal to 3.0, 4.0 and 6.0. In: (a) $d_p = 15$ μm; in (b) $d_p = 30$ μm; in (c) $d_p = 50$ μm; in (d) $d_p = 100$ μm. The curves 1, 2 and 3 in all cases denote the following: $1 \equiv n_T = 3.0$; $2 \equiv n_T = 4.0$; $3 \equiv n_T = 6.0$.

the magnitudes of the column length, L, and of the pore connectivity, n_T, increased. In preparative chromatography, it is desirable to obtain high throughputs within acceptable pressure gradients and this may require the employment of larger diameter adsorbent particles. In such a case, larger column lengths satisfying acceptable pressure gradients with adsorbent particles having higher pore connectivity values could provide high dynamic adsorptive capacities. It is worth noting here that high throughputs and high dynamic adsorptive capacities can be realized in column systems employing large diameter adsorbent particles having fractal pores (fractal particles) [1,2,11–15]; such particles

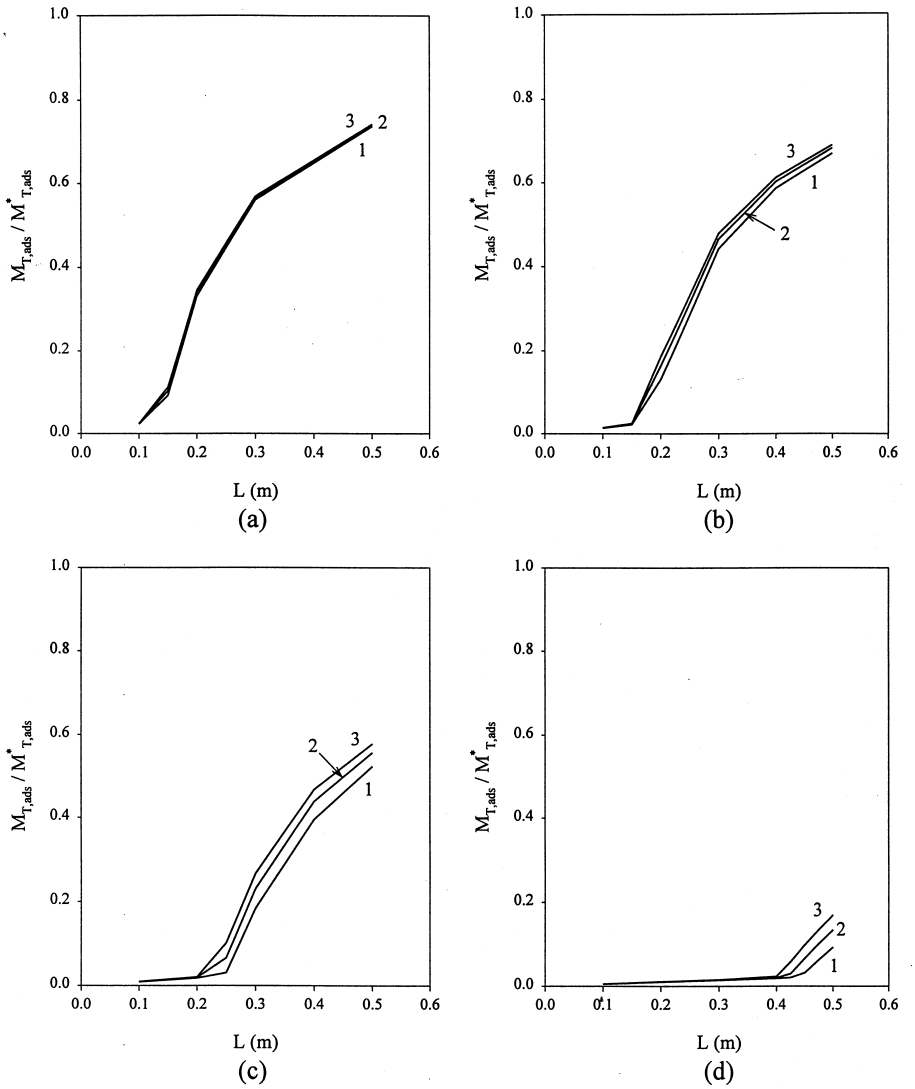

Fig. 9. Dynamic adsorptive capacity, $M_{T,ads}/M^*_{T,ads}$, of the column at time t_b when 5% breakthrough [$C_d(t = t_b, x = L)/C_{d,in} = 0.05$] occurs as a function of the column length, L, at a superficial fluid velocity, V_f, of 500 cm/h for particle diameters, d_p, of 15 μm, 30 μm, 50 μm and 100 μm with the pore connectivity, n_T, equal to 3.0, 4.0 and 6.0. In: (a) $d_p = 15$ μm; in (b) $d_p = 30$ μm; in (c) $d_p = 50$ μm; in (d) $d_p = 100$ μm. The curves 1, 2 and 3 in all cases denote the following: $1 \equiv n_T = 3.0$; $2 \equiv n_T = 4.0$; $3 \equiv n_T = 6.0$.

have high pore connectivity, n_T, and could also allow intraparticle fluid flow. It is also useful to mention here that an alternative chromatographic mode of operation could be to employ monoliths instead of columns packed with porous particles; it has been shown [3] that monoliths could provide higher throughputs and dynamic adsorptive capacities than packed beds of particles, and therefore, an alternative system that could be useful in practice could be the employment of large scale monoliths if such monoliths could be made to be reproducible and operationally stable.

5. Nomenclature

A	Adsorbate
$C_{d,in}$	Concentration of adsorbate A at the column inlet, kg m^{-3} of bulk fluid
C_d	Concentration of adsorbate in the flowing fluid stream in the column, kg m^{-3}
C_p	Concentration of adsorbate A in the fluid of the pores of the adsorbent particle, kg m^{-3} of pore fluid
C_s	Concentration of adsorbate A in the adsorbed phase of the adsorbent particle, kg m^{-3} of adsorbent particle
C_T	Maximum equilibrium concentration of adsorbate A in the adsorbed phase of the adsorbent particle, kg m^{-3} of adsorbent particle
D_p	Pore diffusion coefficient of adsorbate A in the porous adsorbent particle, m^2 s^{-1}
D_L	Axial dispersion coefficient of adsorbate A, m^2 s^{-1}
D_{mf}	Free molecular diffusion coefficient of adsorbate A, m^2 s^{-1}
d_p	Diameter of adsorbent particle, m
d_{pore}	Diameter of pore, m
$f(d_{pore})$	Number of pores of diameter d_{pore}
k_1	Rate constant in Eq. (1) and Eq. (2), m^3 kg^{-1} s^{-1}
k_2	Rate constant in Eq. (1) and Eq. (2), s^{-1}
K	Equilibrium constant ($K=k_1/k_2$)m^3 kg^{-1}
K_f	Film mass transfer coefficient of adsorbate A, m s^{-1}
L	Length of column, m
$M_{T,ads}$	Total amount of adsorbate A in the adsorbed phase of the packed bed at 5% breakthrough, kg
$M^*_{T,ads}$	Total amount of adsorbate A in the adsorbed phase of the packed bed if the concentration, C_s, of the adsorbate in the adsorbed phase was in equilibrium with the concentration, $C_{d,in}$, of the adsorbate in the fluid phase entering the packed bed, kg
n_T	Pore connectivity, dimensionless
PSD	Pore size distribution
r	Radial distance in porous adsorbent particle, m
r_p	Radius of porous adsorbent particle, m
t	Time, s
t_b	Time at which 5% breakthrough occurs, s
v_D	Diffusional velocity in the porous adsorbent particles, m s^{-1}
V_f	Superficial fluid velocity, m s^{-1}
x	Axial distance in column, m

Greek symbols

α_1	Effective molecular radius of β-galactosidase, m
ϵ	Void fraction in column, dimensionless
ϵ_p	Porosity of the porous adsorbent particle, dimensionless
θ	Fractional saturation of adsorption sites, dimensionless

Acknowledgements

The authors gratefully acknowledge partial support of this work by Monsanto.

References

[1] J.J. Meyers, A.I. Liapis, J. Chromatogr. A 827 (1998) 197.
[2] J.J. Meyers, A.I. Liapis, J. Chromatogr. A 852 (1999) 3.
[3] A.I. Liapis, J.J. Meyers, O.K. Crosser, J. Chromatogr. A 865 (1999) 13.
[4] A.I. Liapis, B.A. Grimes, J. Chromatogr. A 877 (2000) 181.
[5] B.A. Grimes, J.J. Meyers, A.I. Liapis, J. Chromatogr. A 890 (2000) 61.
[6] M.A. McCoy, A.I. Liapis, J. Chromatogr. 548 (1991) 25.
[7] O.K. Crosser, Internal Report Number 5, Department of Chemical Engineering, University of Missouri–Rolla, Rolla, MO, 2000.
[8] D. Stauffer, A. Aharony, Introduction to Percolation Theory, 2nd Edition, Taylor and Francis, London, 1992.
[9] G.A. Heeter, A.I. Liapis, J. Chromatogr. A 796 (1998) 157.
[10] N.W. Carlson, J.S. Dranoff, in: A.I. Liapis (Ed.), Proceedings of the 2nd International Conference on Fundamentals of Adsorption, Engineering Foundation, New York, 1987, p. 129.
[11] A.I. Liapis, Math. Modell. Sci. Comput. 1 (1993) 397.
[12] G.A. Heeter, A.I. Liapis, J. Chromatogr. A 711 (1995) 3.
[13] G.A. Heeter, A.I. Liapis, J. Chromatogr. A 734 (1996) 105.
[14] G.A. Heeter, A.I. Liapis, J. Chromatogr. A 743 (1996) 3.
[15] G.A. Heeter, A.I. Liapis, J. Chromatogr. A 760 (1997) 55.